Study of Seismic Capacity of Masonry Infilled Reinforced Concrete Frames Considering the Influence of Frame Strength

Hamood Al-Washali – Ph.D. Candidate, Graduate School of Engineering, Tohoku University, Hamood@rcl.archi.tohoku.ac.jp

Kiwoong Jin – Assistant professor, PhD, Professor, Graduate School of Engineering, Tohoku University, Jin@rcl.archi.tohoku.ac.jp

Masaki Maeda – Professor, PhD, Professor, Graduate School of Engineering, Tohoku University, Maeda@rcl.archi.tohoku.ac.jp

Abstract: Unreinforced masonry infilled-RC frames are widely used in many developing countries. Even though the influence of the masonry walls on the behavior of structure was recognized from the experience of past earthquake disasters, but many practicing engineers still assume that the infill walls are non-structural walls due to incomplete knowledge of the behavior of such structures. In addition, modelling and estimating strength of masonry infill commonly considers only the material characteristics of masonry and ignoring confining influences of boundary frame. In this paper, first, an experimental study on RC frame with unreinforced masonry infill considering the influence of boundary frame strength on their seismic capacity. The results showed that shear strength and deformation capacity of masonry infill greatly improved by increasing the strength of boundary frame. Second, the investigation of strength, ductility and stiffness based on experimental results and comparative study with existing methods that are commonly used.

Keywords: Reinforced concrete buildings, Masonry infill, Seismic capacity, Boundary frame strength.

1. Introduction

Many of the reinforced concrete buildings in the world and particularly in developing countries use masonry infill as partition walls. The influence of masonry on the structural behavior was recognized from the experience of earthquake disasters and experiments by several researchers (i.e., priestly et al. 1992). In general, masonry infill increases the frame strength, which is considered as a beneficial point. On the other hand, masonry infill exerts reaction forces on the RC frame causing additional moment and shear forces, which results in unexpected failure modes FEMA 306 (1998). In addition, the masonry infill greatly increases the frame stiffness that might changes the seismic demand due to significant reduction in natural period of the building. Despite of these distinctive characteristics, many practicing engineers still assume that the walls are non-structural elements due to incomplete knowledge concerning RC frames with masonry infill behavior and complexity in evaluating their failure modes. The seismic performance of masonry infill depends on several parameters such as the confinement effect, masonry type, aspect ratio, mortar strength, etc. Among these factors, the strength of boundary RC frame is a crucial parameter that not only governs the behavior and failure modes of the RC frame but also the masonry infill strength and failure mode, as shown in previous experiments conducted by Mehrabi et al. (1996). However, modelling and estimating strength of masonry infill commonly considers only the material characteristics of masonry and ignoring confining influences of boundary frame.

In brief, the influence of boundary frame strength and its influence on the seismic capacity infill and the overall frame have not been clearly identified. Thus, the objective of this paper is as follows: First, the experimental investigation of RC frame with unreinforced masonry infill is carried out with in-plane cyclic loading tests, where the only varying parameter is the lateral strength of surrounding frames. Second, the investigation of strength, ductility and stiffness based on experimental results and comparative study.

2. Experimental program

2.1. Test specimens

Two half-scaled specimens with different RC frames, having same unreinforced masonry infills, are designed. The main variance parameter for test specimens is the ratio of the boundary frame to masonry infill lateral strength defined as β index, as shown in Eq. (1). Specimens are named WF (weak frame) and SF (strong frame) with β of 0.4 and 1.5, respectively.

$$\beta = V_f / V_{inf} \tag{1}$$

Where V_f is the boundary frame lateral strength which is calculated to be the ultimate flexural capacity of a bare frame with plastic hinges at top and bottom of columns. The V_{inf} is the masonry infill lateral strength calculated based on Eq. (2) which is a simplified empirical equation showing good agreement with experimental database studied by the author (Al-Washali et al. 2017)

$$V_{inf} = 0.05\, f_m \cdot t_{inf} \cdot l_{inf} \tag{2}$$

Where f_m is the compressive strength of masonry prism, t_{inf} is the infill thickness, l_{inf} is the infill length.

The specimen dimensions and details are shown in Figure 1. Both specimens are identical except for the column size and reinforcement, as shown in Figure 1. The beams were designed to be stronger and stiff enough to simulate a typical case of a weak column and strong beam system observed in existing buildings of old designs.
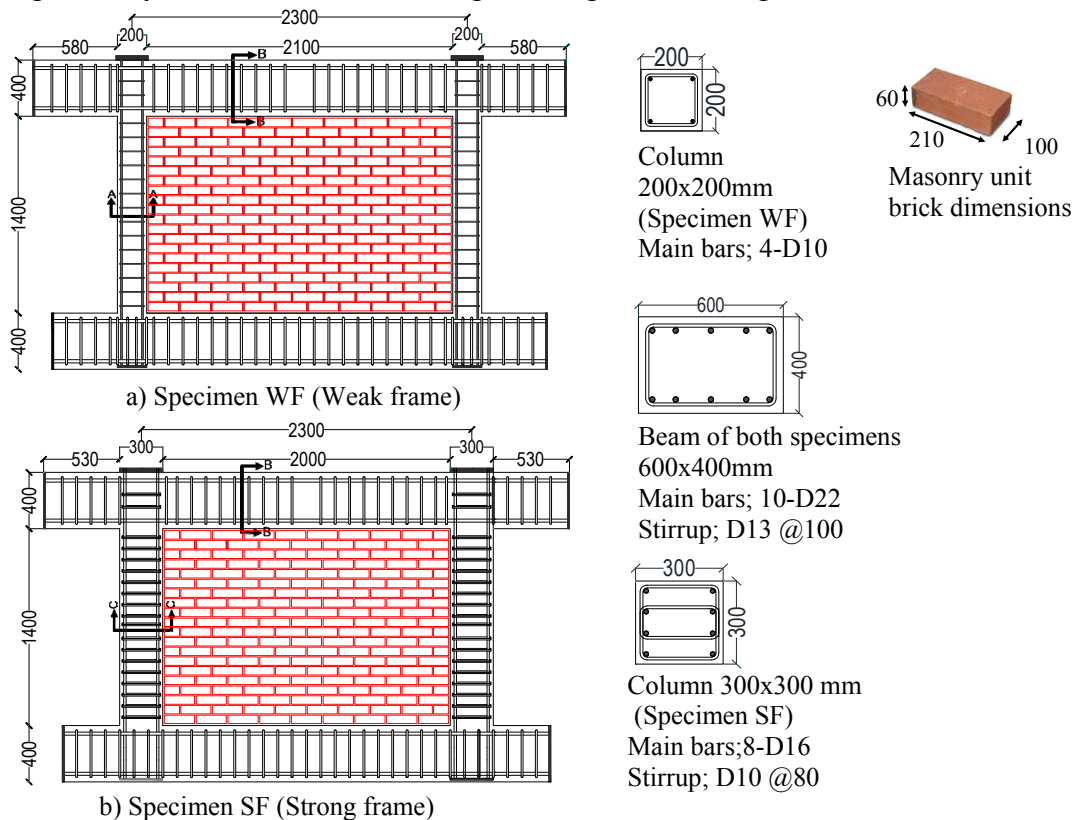

a) Specimen WF (Weak frame)

Column
200x200mm
(Specimen WF)
Main bars; 4-D10

Masonry unit
brick dimensions

Beam of both specimens
600x400mm
Main bars; 10-D22
Stirrup; D13 @100

Column 300x300 mm
(Specimen SF)
Main bars;8-D16
Stirrup; D10 @80

b) Specimen SF (Strong frame)

Fig. 1.Dimensions and reinforcement of specimens; units in mm

2.2. Material properties

The infill panels are constructed using 60 x 100 x 210 mm solid bricks conventionally used in Japan. A professional mason built the infill, after the frame construction, where its thickness is 100mm and mortar head and bed joint thickness is about 10mm. Tables 1 and 2 show the material properties based on material tests where the values represent the mean values of three samples. The masonry prism strength is the masonry prism compressive strength tested according to ASTM C1314 [6]. The material tests were conducted at the same time with the experimental loading for each specimen individually.

Table 1. Material properties of Concrete and Masonry details

Specimen name	Frame Concrete			Masonry Prism			Mortar compress -ive strength	Compress -ive strength of brick unit (Mpa)
	Compress -ive strength (MPa)	Elastic modulus (MPa)	Split Tensile strenght (MPa)	Compress -ive strength (MPa)	Elastic modulus (MPa)	Strain as peak stress		
WF	24.2	2.3×10^4	2.1	17.3	7840	0.00375	20.2	38.1
SF	28.3	2.3×10^4	2.4	18.6	8140	0.00388	30.6	38.1

Table 2. Reinforcement mechanical properties

Bar	Nominal strength	Yield strength (MPa)	Ultimate tensile strength (MPa)
D6	SD345	476	595
D10	SD345	384	547
D13	SD345	356	555
D16	SD345	370	556
D22	SD390	447	619

2.3. Test setup and instrumentation

The loading system are shown schematically in Figure 2. The vertical load was applied on RC columns by two vertical hydraulic jacks and was maintained to be 200kN on each column. Two pantograph, attached with the vertical jacks, restricted any torsional and out-of-plane displacement. Two horizontal jacks, applying together an incremental cyclic loading, were attached at the beam level and were controlled by a drift angle of R%, defined as the ratio of lateral story deformation to the story height measured at the middle depth of the beam (h=1,600mm). The lateral loading program consisted of 2 cycles for each peak drift angle of 0.05%, 0.1%, 0.2%0.4%, 0.6, 0.8%, 1%, 1.5% and 2 %.
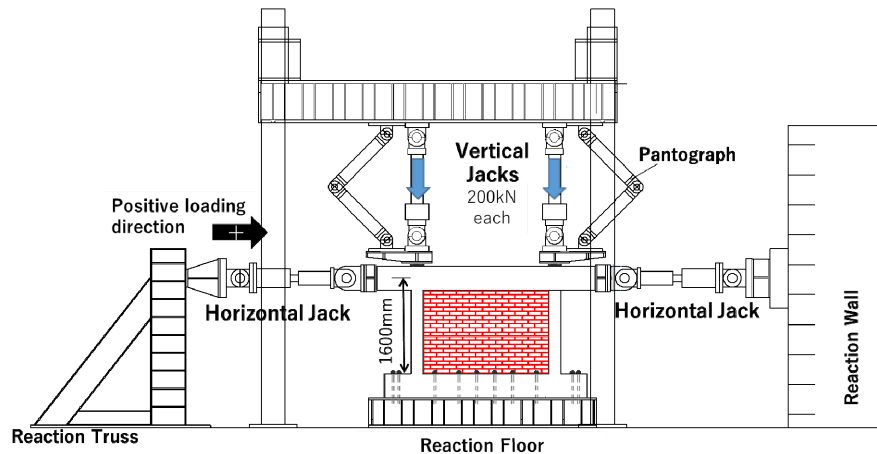

Fig. 2. Test setup (units: mm)

2.3. Experimental results

The lateral load versus story drift angle of both specimens are shown in Figures 3 and 4. Cracks and failure patterns after final drift cycle of 2.0% are shown in Figure 5.

For Specimen WF:

very small cracks on mortar bed joint and diagonal cracks on bricks near loading corner of infill panel, less than 0.3mm width, started at early stages of loading just when the drift angle was 0.05%. At drift angles of 0.2% and 0.4%, the longitudinal reinforcement in the tensile column (windward column) yielded at the upper critical section and above its mid-height, respectively, forming failure mechanism similar to a short column, as illustrated in Figure 6-a). Just after reaching the maximum lateral strength, there was a sudden drop of lateral load bearing capacity with extensive cracking and spalling of bricks. After the drift of 1%, the main failure mechanism from diagonal cracks changed to sliding cracks, and clear sliding movement at the mid-height of the infill was noticed. At drift story of 2% in the negative cycle, the concrete around the reinforcement of top compression column spalled-off and main bars buckled.

For Specimen SF:

Cracking of infill panel also started at the peak of the first loading cycle, which was relatively similar to the crack width observed in specimen WF at this stage. At drift angles between 0.6% ~ 0.7%, both columns yielded at the locations shown in Figure 6-b). As it reached its maximum strength, the lateral load gradually degraded (contrarily to the sudden degradation of strength in previous specimen WF) with the drift angle increase until the drift angle of 1.5%, where there was a slight drop of the lateral load, after the horizontal sliding between bricks clearly increased. At the drift angle of 2%, the loading stopped as planned, and the masonry infill damage at this point was much greater than observed in the previous specimen WF (see Figure 5). In spite that columns had many cracks, there was no extensive damage or spalling of concrete cover.
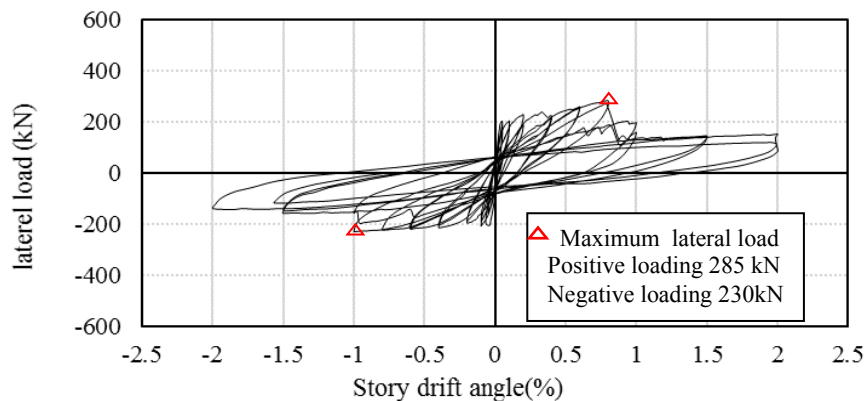
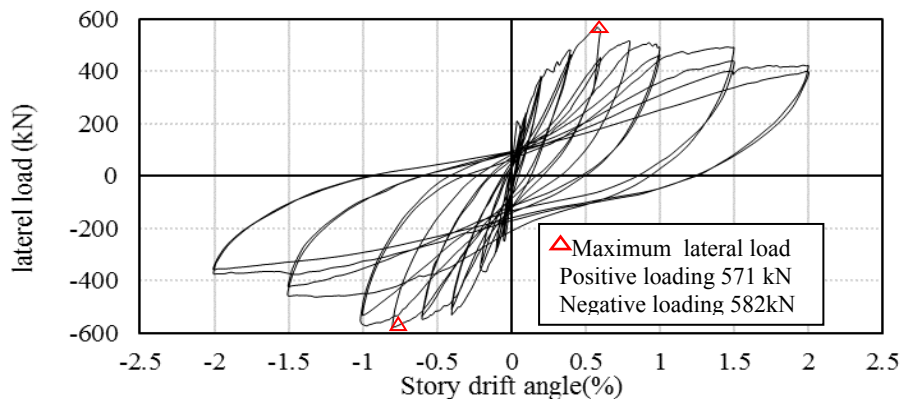Fig. 3 - Lateral strength & story drift angle for specimen WF

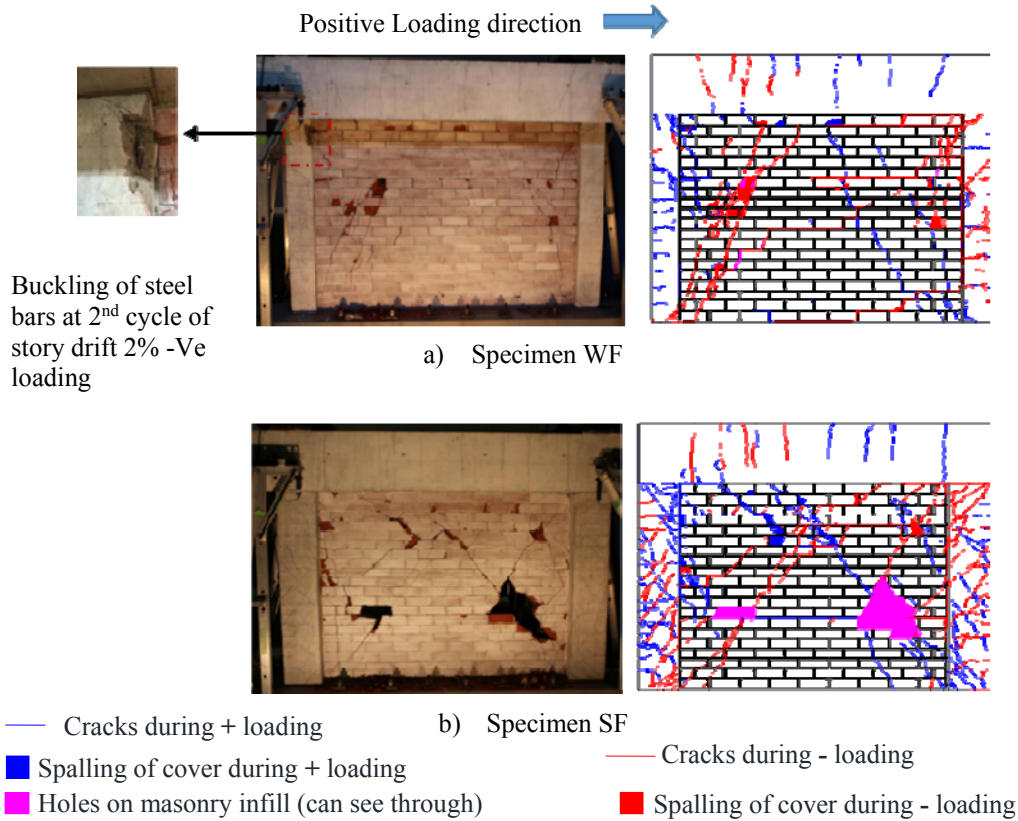Fig. 4 - Lateral strength & story drift angle for specimen SF

Positive Loading direction

Buckling of steel bars at 2nd cycle of story drift 2% -Ve loading

a)   Specimen WF

b)   Specimen SF

—— Cracks during + loading

—— Cracks during - loading

■ Spalling of cover during + loading

■ Spalling of cover during - loading

■ Holes on masonry infill (can see through)

Fig. 5   Crack patterns observed at end of the test: a) specimen WF b) Specimen SF

Main bars yielded at drift 0.2%

Main bars yielded drift 0.4%

Main bars yielded at drift 0.6%~0.7%

1000 mm

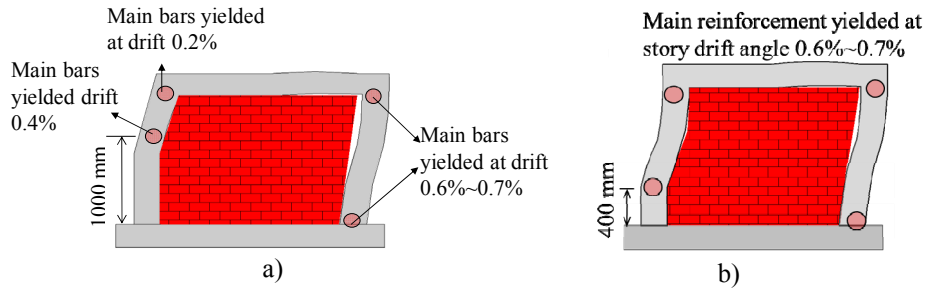Main reinforcement yielded at story drift angle 0.6%~0.7%

400 mm

a)

b)

Fig. 6.   Hinge locations formed in RC frame a) specimen WF   b) Specimen SF

3. Discussion of experimental results:

3.1 Lateral strength:

The maximum lateral load contributed by the masonry infill (V_{inf}) is calculated by deducting the bare frame lateral strength (V_f) from the maximum lateral load of the overall structure (V_{max}), as shown in Equation (3):

$$Vf=4Mu/H \qquad (3)$$

$$V\inf = V\max - Vf \qquad (4)$$

Where Mu is the minimum plastic moment of the column or beam calculated by AIJ provision (2010) and H is the clear height of column (taken here as infill height).

Table 1 shows the experimental shear strength of masonry infills in both specimens, which is the shear force (V_{inf}) divided by the infill cross-sectional area. Even though both infill panels are made by exactly same material and have similar prism compression strength, specimen SF has the shear capacity of 1.48N/mm^2 which is about 1.5 times the shear strength in specimen WF (0.93 N/mm^2).

Table 3. Maximum lateral load and shear strength of infill

specimen name	Vf (kN)	Experiment V_{inf} (kN) using		Maximum τ_{inf} (N/mm^2)		Average Experiment V_{inf} of both directions (N/mm2)	Average of shear strength τ_{inf} both directions (N/mm2)
		Positive loading	Negative loading	Positive loading	Negative loading		
WF	71	211	159	1.06	0.80	185.0	0.93
SF	280	291	302	1.46	1.51	296.5	1.48

3.1.1 Comparison of lateral strength with previous literature

The in-plane capacity of the masonry infill depends mainly on the type of failure mechanism. The failure mechanism types and identification are different between building standards or researchers. The most recognized failure modes are diagonal compression failure and sliding shear failure modes. The failure mechanism observed in experimental results as mentioned earlier, is a mixture of both: compression and sliding failure. In this study, Table 4 shows the comparison of the infill strength with following methods: Diagonal compression and sliding equation by FEMA 306 (1996), Liauw et al. (1985) method, Flanagan et al. (1999) method, Paulay et al (1992) method for sliding strength and simplified equation presented by author in previous study (Al-Washali et al. 2017).

As shown in Table 4, Liauw et al. (1985) method and simplified method of Flanagan et al. (1999) greatly overestimate the strength. The methods proposed to calculate sliding capacity by FEMA 306 (1996), and Paulay et al. (1992) greatly underestimate the infill strength. Diagonal compression strength by FEMA 306 (1996) and the simplified equation by AlWashali et al. (2017) showed relatively good estimation for specimen WF, but it underestimated that of Specimen SF. This underestimation is considered due to the ignorance of the confinement effect of the strong boundary frame.

Table 4 Ratio Experimental peak strength/Analytical strength

Test specimen	FEMA 306 (1996) (Compre--ssion)	Liauw et al. (1985)	Flangan et al. (1999)	FEMA 306 (1996) (Sliding)	Paulay et al (1992) (Sliding)	Simplified method AlWashali et al. (2017)
Specimen WF	1.21	0.69	0.50	3.14	1.58	1.18
Specimen SF	1.41	0.81	0.66	6.26	2.13	1.62
Average	**1.31**	**0.75**	**0.58**	**4.70**	**1.85**	**1.40**

3.2 Stiffness:

The initial stiffness K_o of infilled frame is taken as the slope between the origin point of the load-displacement curve and the point with the major visible crack in the masonry infill and the RC frame, which was determined as the story drift of 0.1%.

Table 3 shows the comparison between the initial stiffness of overall frames and that of bare frames. Herein, the initial stiffness of bare frame is calculated based on its elastic gross concrete section. The masonry infill greatly increased the initial stiffness up to about 7.1 times that of bare frame in specimen WF. Therefore, in the seismic design, ignoring the contribution of masonry infill to stiffness and natural period of building may cause non-conservative design practice since buildings with lower natural period have greater seismic forces.

The most well recognized method for calculating the infill stiffness is using the equivalent diagonal compression strut, which has the same elasticity and thickness with the infill panel. Paulay et al. (1992) recommended using the effective width of strut, where W_{ef} and d_m is the diagonal length of infill panel. in Eq. (5).

$$W_{ef}= 0.25d_m \qquad\qquad (5)$$

Table 5 shows the comparison between experimental and numerical initial stiffness based on the strut width recommended by FEMA 306 (1996) and Pualay et al. (1992). The Strut width calculated by FEMA 306 (1996) underestimates the initial stiffness by about 1.9 and 1.08 for specimen WF and specimen SF, respectively. On the other hand, Eq. (3) recommended by Paulay et al. (1992) agrees pretty well with specimen WF by the ratio of 0.94, but overestimated specimen SF by the ratio of 1.36. Based on these results, make a proposed assumption of the strut width W_{ef} to be $0.2dm$ (d_m : diagonal length) gives relatively good estimation for the initial stiffness.

Table 5. Comparison of analytical and experimental initial stiffness

| Specimen | Exp. stiffness | Calculated stiffness | | | | | | | |
| | | Bare frame | | Initial stiffness using diagonal strut model | | | | | |
	Initial stiffness (kN/mm)	Initial stiffness (kN/mm)	Ratio	FEMA 306 (1996) (kN/mm)	Ratio	Paulay et al (1992) (kN/mm)	Ratio	Proposed W_{ef}=0.2d$_m$	Ratio
WF	128	18	7.07	68	1.90	136	0.94	114	1.13
SF	150	79	1.91	139	1.08	205	0.73	180	0.84
Average			4.49		1.49		0.84		0.98

Note : *Raio = experimental / Analytical

3.3 Deformation capacity:

In this study, a backbone curve for RC frames with masonry infills is suggested as shown in Figure 7. R_{-crack}, R_{-max} and R_u are the representative drift angles at the cracking, the maximum strength and the strength degradation point, respectively, where the strength degradation point is set to be 80% of the maximum strength.
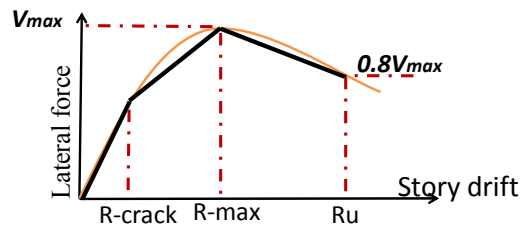

Fig..7 Idealization of backbone curve

The simplified backbone curves for specimens WF and SF are shown in Figure 8. R-crack and R_{-max} is estimated to be 0.1% and 0.8% for both specimens . For R_u, it was found to be 0.9% and 1.6% for specimen WF and SF, respectively. Therefore, it can be concluded that the influence of surrounding frame strength on R_{-crack} and R_{-max} was slight, but greatly alters the strength degradation slope and R_u. The smooth decrease of strength and improvement of ductility for specimen SF are considered to be due to the confinement by the stronger surrounding frame, which reduces the inelastic deformation of masonry infill.
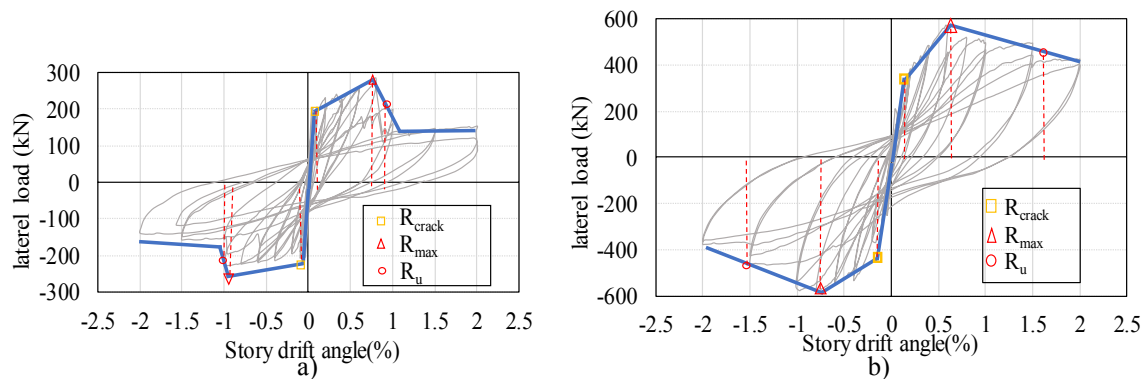
Fig..8 Backbone curve & deformation limits: a) Specimen WF   b) Specimen SF

4. Conclusions

Experimental results to investigate the seismic capacity of unreinforced masonry infilled-RC structure was presented. Based on this study results, the following conclusions can be drawn:

a) Increasing the ratio of the frame to masonry infill lateral strength named β, greatly improved the infill strength. However, most methods proposed to estimate the infill lateral strength, by previous researchers, underestimate or ignore the influence of β.

b) The initial stiffness of both frames were almost similar until story drift angle of 0.1%, which is considered the major cracking point. After drift story of 0.1%, the stiffness of both specimens degraded rapidly. Assuming diagonal strut width to be 0.2 times diagonal length gives relatively good estimation of initial stiffness in both specimens.

c) Drift angles R_{crack} (cracking point) and R_{max} (story drift at maximum strength) was not much influenced by parameter of boundary frame strength. However, R_u drift (degradation point of 80% of maximum strength) was greatly improved by the confinement of stronger columns.

Acknowledgements

References

Al-Washali H, Suzuki Y, Maeda M. Seismic Evaluation of Reinforced Concrete Buildings with Masonry Infill Wall. *The 16th World Conference of Earthquake Engineering*, Chile, 2017.

American Society of Testing and Materials (ASTM). *Standard Test Method for Compressive Strength of Masonry Prisms.* ASTM C1314, West Conshohocken, PA., 2011.

Architectural Institute of Japan (AIJ). *AIJ Standard for Structural Calculation of Reinforced Concrete Structures*. 2010.

FEMA 306. *Evaluation of Earthquake Damaged Concrete and Masonry Wall Buildings – Basic Procedures Manual.* Report No. FEMA 306 (ATC-43 Project), 1998.

Flanagan RD, Bennett RM. In-Plane Behavior of Structural Clay Tile Infilled Frames. *Journal Structural Engineering,* Vol. 125, No.6,1999, pp 590–599.

Liauw TC, Kwan KH, Unified Plastic Analysis for Infilled frames. *Journal of Structural Engineering*, Vol 111, No.7. 1985, pp 1427-1448.

Mehrabi AB, Shing PB, Schuller M, Noland J. Experimental Evaluation of Masonry-infilled RC Frames. *Journal of Structural Engineering, ASCE*, Vol. 122, No. 3, March 1996.

Paulay T, Priestley MJN. *Seismic Design of Reinforced Concrete and Masonry Buildings.* John Wiley & Sons; 1992.